

Feedback control of optical beam spatial profiles using thermal lensing

Zhanwei Liu^{†,1} Paul Fulda^{2,*} Muzammil A. Arain^{†,3} Luke Williams² Guido Mueller² David B. Tanner² and David H. Reitze^{2,4}

¹*School of Applied and Engineering Physics, Cornell University
Ithaca, New York 14850, USA*

²*Department of Physics, University of Florida, P.O. Box 118440,
Gainesville, Florida 32611, USA*

³*KLA-Tencor Company, One Technology Drive, Milpitas, California 95035, USA*

⁴*Currently: LIGO Laboratory, California Institute of Technology, MS 100-36,
Pasadena, California 91125, USA*

compiled: October 29, 2018

A method for active control of the spatial profile of a laser beam using adaptive thermal lensing is described. A segmented electrical heater was used to generate thermal gradients across a transmissive optical element, resulting in a controllable thermal lens. The segmented heater also allows the generation of cylindrical lenses, and provides the capability to steer the beam in both horizontal and vertical planes. Using this device as an actuator, a feedback control loop was developed to stabilize the beam size and position.

1. Introduction

High laser powers in scientific experiments and industrial applications often lead to the generation of thermal lenses in optical systems, causing unwanted changes in spatial beam profiles. Absorption of high-power laser radiation in transmissive optical materials deposits heat in a non-uniform spatial distribution, leading to a temperature gradient and therefore refractive index gradient across the optic surface. The resulting thermal gradient index lens changes the spatial mode of the laser and can cause aberrations which lead to modal distortions [1–3].

We report the development of an active device designed to counteract the effects of thermal lensing, first described in Ref. [4]. Four individually addressable heating elements are used to generate thermal gradients across a transmissive optical element, resulting in a controllable thermal lens having

both spherical and (if necessary) cylindrical components, providing the capability to focus and steer the beam. In this article we demonstrate the use of this device as an actuator in a beam shaping feedback loop, operating over a wide non-linear range to correct for impulsive thermally generated beam distortions.

While potential applications of such an adaptive device exist in areas of laser material processing [5], image processing [6, 7], and optical displays [8], this work is focused mainly on applications to Advanced LIGO (aLIGO), a high power laser interferometer which aims to detect gravitational waves from merging neutron stars, black holes and other astrophysical sources [9].

The aLIGO pre-stabilized laser system generates a 200 W laser beam at 1064 nm [10]. This high power beam is expected to create thermal lenses in many of the optics comprising the detector. In turn, this thermal lensing causes a laser power dependence in the mode matching between the beam from the pre-stabilized laser and the various optical cavities present in the interferometer. In particular, the mode matching between the beam transmitted through the input mode cleaner and the main inter-

* Corresponding author: pfulda@phys.ufl.edu

[†]This work was performed when these authors were based at the University of Florida

ferometer power recycling cavity is expected to be dependent on the laser power [11]. A system which can be used to correct for the power dependence is therefore highly desirable in order to maintain good mode matching into the interferometer. For this application, where repositioning of lenses is not easily achieved due to the ultrahigh-vacuum environment, adaptive optical elements present the most practical solution for maintaining optimal beam parameters in the high laser power regime.

The device presented here is not the first method developed to compensate thermal lenses; there are a number of thermal compensation techniques, using for example negative thermo-optic coefficient materials [12], CO₂ laser heating and electrical heating of the optical elements [13, 14], tunable liquid crystals [6] or deformable mirrors [15]. However, this device is vacuum compatible and high laser power compatible, as well as being versatile and reliable. Vacuum and high laser power compatibility are essential for use of the device in aLIGO, where it may be employed within the ultrahigh-vacuum system and will be required to transmit the full science laser power.

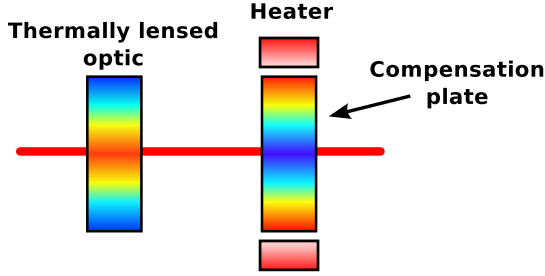


Figure 1: The conceptual design of thermal compensating system. The heated compensation plate is used to compensate the laser induced thermal lens.

The basic principle of the adaptive spatial mode control method is shown in Fig. 1. The Gaussian

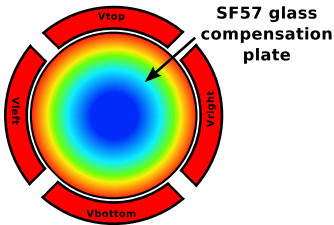


Figure 2: The design of the compensation plate. The SF57 glass is heated by four independent heaters to produce the required thermal profile.

profile of the science laser beam creates a power-dependent thermal lens in a transmissive optic. A thermal compensation plate which can be heated from the outside with four individual heaters is placed after the transmissive optic. When all four heaters are heated equally, the defocusing thermal gradient index lens that is created in the compensation plate can compensate the focusing thermal lens generated in the transmissive optic. The use of four individual heaters instead of just one ring heater enables greater control over the heating profile, allowing for the correction of astigmatic thermal lenses and also providing beam steering capabilities.

In practice, the thermal compensation system will have to correct for non-stationary thermal effects, as the circulating laser power may change during the operation of the interferometer. To this end, the thermal compensation should be applied as part of a feedback loop, where any unwanted changes in the spatial beam profile are detected, processed, and compensated automatically.

2. Experimental method

The compensator was realized in our experiment using the four segmented heater (FSH) shown in figure 2, and described in Ref. [4]. SF57 glass was chosen for the substrate because of its large thermal expansion and thermo-refractive ($\frac{dn}{dT}$) coefficients, which give the device a large dynamic range of achievable focal lengths. The four heating segments each consist of a resistive heater on Kapton film with a resistance about of 25 Ω , and are each supplied by a current source, delivering a maximum current of 1.5 A. This setup allows us to tune the focal length in the range from effectively minus infinity to -10 m.

A simplified experimental arrangement is shown in Fig. 3. Light from a 200 mW Nd:YAG laser is passed through the first adaptive optic, referred to henceforth as the *aberrator*, which is used to simulate the thermal lensing effect which is to be compensated. The beam transmitted through the aberrator is then passed through the second adaptive optic, henceforth referred to as the *compensator*, which is used to compensate for the actions of the aberrator. Since the laser power in the setup was not sufficient to produce a significant thermal lens, the process of thermal lensing was emulated in another way. Initially the aberrator was strongly biased by radially heating, such as to produce a negative focal length lens. A reduction in the radial heating of the aberrator from this level, and hence

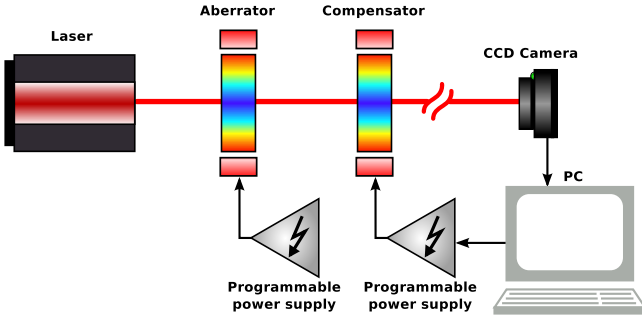


Figure 3: A simplified experimental setup of the compensating system. Both the aberrator and compensator are FSHs. The aberrator was used to emulate a laser heating induced thermal lens. A feedback system was employed to drive the heaters in the compensator such as to maintain the original beam parameters, as measured at the CCD.

reduction in the power of thermal lens produced, was used as an analogue for an increase in central heating that would be caused by a high power laser beam. The beam radius at the aberrator was about 1.5 mm ($1/e^2$ intensity).

A Gigabit Ethernet CCD camera [16] was placed further downstream in order to monitor the beam transmitted through the aberrator and compensator. The spot size and lateral position of the beam were calculated from the CCD data, and used as a reference relative to which deviations could be measured and corrected. After processing the data, four output signals are generated; the beam radius and centroid position on the horizontal and vertical axes. These signals are used to control the four heating voltages on the FSH in four directions.

In order to control the heating-induced thermal lens profile of the compensator accurately, it was necessary first to characterize the response of the compensator to actuation of each of the four heating elements. Differences in the mechanical contacts between the heaters and the glass, as well as between the heaters and the mount, can lead to different responses of the compensator to each heater. To map out the asymmetries in the compensator actuation, the beam first was centered on the CCD while all the heating elements were turned off. The voltage applied to the top heating element was steadily increased, and the other three voltages were adjusted in order to re-center the beam on the CCD. This measurement represents a relative calibration of the four different heaters, because unequal heating by the four heaters will lead to a change in the align-

ment of the transmitted beam. The bias voltages obtained when the top heating element was supplied with 5 V were 4.96 V, 5.44 V and 6.29 V for the left, right and bottom heaters respectively.

The response of the optical elements to the applied heating is far from linear over their full actuation range. In order to use the full range in a feedback loop it was therefore necessary to make a look up table, which was used to adjust the feedback filters to each heater for each set of heater DC offset voltages. Offset voltages were applied to each of the heaters in order to explore the measured beam size parameter space. These DC offsets were chosen such as to provide symmetric heating, as this was the actuation regime of primary interest in this experiment. The DC offsets required to reach specific regions within this space were recorded. At each of these points, transfer functions from applied voltage to measured beam parameter deviation were measured for each heater.

The applied signal amplitude for the transfer functions was ± 0.3 V; small enough to be within the linear range of the actuator. At 1 mHz this linear range corresponds to a beam width deviation of around $7 \mu\text{m}$ and a beam centroid position deviation of around $3 \mu\text{m}$. Each element in the look up table was then composed from the DC bias offset values required to bring the beam parameters *close* to the working point, and the transfer functions from applied signal to beam parameter deviation within the linear range in order to bring the beam parameters to the precise working point. Figure 4 shows the fitted 3-pole transfer function from each heater to the corresponding beam parameters for one set of DC voltage values from the look up table.

These transfer functions were used to describe the system in term of its transfer matrix:

$$\begin{bmatrix} \Delta w_H \\ \Delta p_H \\ \Delta w_V \\ \Delta p_V \end{bmatrix} = \begin{bmatrix} M_{11} & M_{12} & M_{13} & M_{14} \\ M_{21} & M_{22} & M_{23} & M_{24} \\ M_{31} & M_{32} & M_{33} & M_{34} \\ M_{41} & M_{42} & M_{43} & M_{44} \end{bmatrix} \begin{bmatrix} \Delta V_{\text{left}} \\ \Delta V_{\text{right}} \\ \Delta V_{\text{top}} \\ \Delta V_{\text{bottom}} \end{bmatrix}, \quad (1)$$

where w and p represent beam width and position respectively, and the subscripts H and V represent horizontal and vertical directions respectively; ΔV are the small actuation voltages (not the bias voltages) applied to the left, right, top and bottom sections of the FSH; and M is the 4×4 transfer matrix. The control matrix for feedback to the compensator was obtained by inverting this transfer matrix.

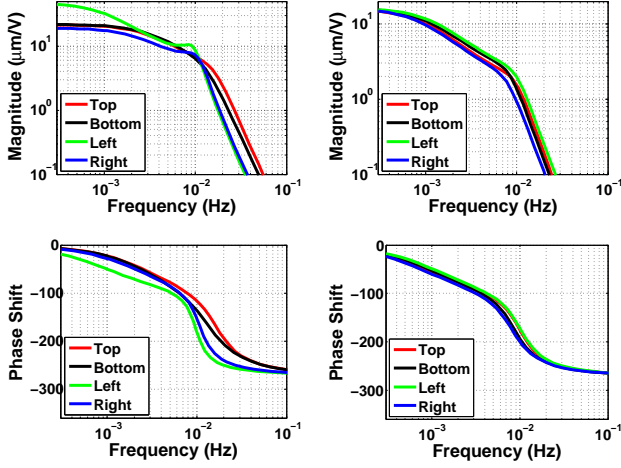


Figure 4: Transfer function of input signals $V(t) = 5 + 0.3 \sin(2\pi ft)$ V on the labelled heating element to beam spot width (left) and centroid position (right). Only the transfer functions from each actuator to its primary actuation axis are shown.

3. Experimental demonstration

3.A. Compensation of constant uniform thermal aberration

In this section we demonstrate feedback compensation for circularly symmetric thermal aberration, such as may be caused by absorption of high laser powers in transmissive optics under normal incidence. The aberrator was uniformly heated at each quadrant until thermal equilibrium was reached, and then the heating power was turned off. The left panel of Fig. 5 shows the temperature profile of the aberrator at thermal equilibrium; in the central part of the optic the induced temperature gradient creates a good approximation to a spherical thermal lens.

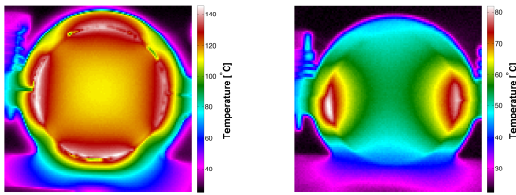


Figure 5: The temperature profile of the aberrator under the symmetric (left) and astigmatic (right) heating conditions.

Figure 6 shows time domain measurements of all 4 of the measured beam parameters while the beam shaping feedback loop was closed. The horizontal

and vertical widths of the beam are different since the available laser output beam is elliptical, and no attempt was made to circularize it. During the run, two impulsive aberrations were generated — one at 90 s (symmetrically reducing the aberrator heating) and one at 860 s (re-applying the aberrator heating). After each impulsive aberration, the parameters recovered to their set-point values within approximately 300 s.

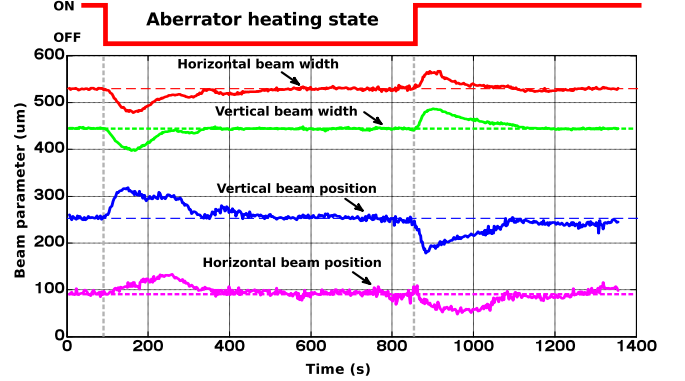


Figure 6: Time series of the measured beam parameters while the beam-shaping feedback loop was closed. Impulsive beam aberrations were applied at 90 s and 860 s.

Initially, as the aberrator cools down and its effective focal length becomes less negative, the beam parameters measured at the CCD begin to change. The beam sizes in both axes decrease at first, as expected due to the change in focal length. The beam spot position in both axes also begins to change; this change may be caused either by imperfect centering of the beam on the aberrator, or by differences in the rate of heat loss from different areas of the aberrator optic. For example, one may expect a greater rate of heat loss through conduction in the the lower portion of the aberrator due to its mechanical contact with the steel post on which it is mounted. This will lead to a linear component in the thermal gradient across the optic, thus causing a shift in the transmitted beam position.

As the beam parameters begin to change, a slow integrator in the feedback signal path determines and applies the bias voltages required to return the beam parameters close to the set-points. During this time a linear proportional-integral controller also applies small signals (within the linear regime), filtered by the transfer matrix elements corresponding to the closest current DC offset voltage look up table elements, to compensate for small deviations in each of the four beam parameters around the

working point. The beam parameters return to the set-point values by around 300 s after the impulsive aberration; the compensation system has regained the starting beam parameters at the CCD, despite the continued presence of the aberration.

3.B. Compensation of astigmatic thermal aberration

In this section we demonstrate the ability of the compensator to correct for astigmatic heating by applying heat in the vertical or horizontal axes only. This experiment was similar to the axisymmetric heating experiment, except that the heating was only applied to the aberrator across the horizontal axis, at the left and right heaters. In the initial state the aberrator was heated astigmatically until it reached thermal equilibrium, producing the temperature profile shown in the right panel of Fig. 5. Three impulsive astigmatic aberrations were then applied by stopping the heating after 420 s, reapplying the heating after 1800 s, and finally ceasing the heating after 2450 s.

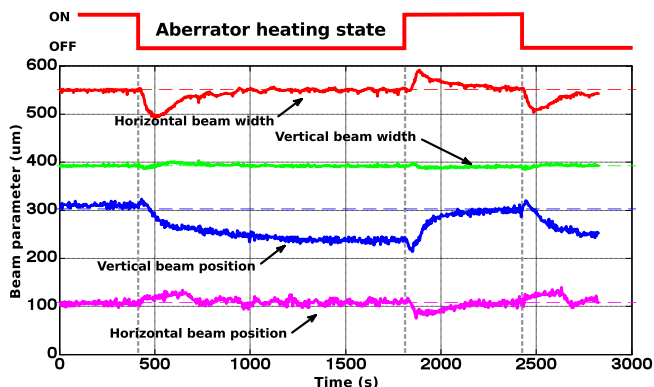


Figure 7: Time series of the measured beam parameters while the beam-shaping feedback loop was closed, for astigmatic aberrations. Impulsive astigmatic beam aberrations were applied at 420 s, 1800 s and 2450 s.

Figure 7 shows the time series of the four measured beam parameters throughout the measurement period. As in Fig. 6, it can be seen that the control loop returns the beam sizes measured at the CCD to their initial set-point values before the impulsive aberrations were applied. However, it is also clear that the beam position along the vertical axis was not well controlled by the feedback loop. When the aberration is first applied the beam drifts lower, and this error is not corrected for by the compensator.

This drift is most likely caused by the fact that the

look up table was only measured for symmetric DC offset values, i.e. those used for symmetric compensation. As a result, it was decided to weight the feedback to beam size more heavily than the feedback to beam position for the astigmatic compensation case. If necessary, a separate look up table could be made for purely astigmatic compensation, and one may consider interpolating between this and the symmetric compensation look up table in order to cover the full range of compensation. In a realistic application of this device, however, alignment drifts such as those observed here can be compensated easily using movable mirrors.

3.C. Noise analysis

As with any feedback loop, it is important to ascertain the level of noise injected into the system as a consequence of implementing the loop. To this end, the standard deviations in beam parameters were calculated with and without actuation on the aberrator. In the state where neither the aberrator nor compensator were heated, the standard deviations in beam radius were 0.15 % and 0.16 % of the mean beam radius in the horizontal and vertical axes respectively, and the standard deviations in beam pointing angle were $0.27 \mu\text{rad}$ and $0.57 \mu\text{rad}$ for the horizontal and vertical axes. In the case where the aberrator was heated with the strong bias voltage, the corresponding standard deviations increased to 0.40 %, 0.33 % and $2.9 \mu\text{rad}$ and $2.1 \mu\text{rad}$. Here it can be seen that even static actuation of the FSHs leads to a significant increase in beam parameter noise. This is almost certainly a consequence of operating the devices in air; the high temperatures at the element ($>100^\circ\text{C}$) cause turbulent air flow in its vicinity resulting in increased jitter downstream. This increased jitter is expected to be strongly mitigated when the actuators are used in vacuum.

4. Conclusions

It has been demonstrated that a segmented heating-compensating system can be used as an actuator in an active feedback loop to correct for time-dependent thermally-induced aberrations of optics. The compensation of both uniform and astigmatic aberrations was tested. The uniform aberration compensation was shown to return all measured beam parameters to their initial values within around 300 s of the application of an impulsive thermal aberration. The astigmatic aberration compensation showed a similar performance for most of the measured beam parameters, although it was

unable to compensate for a drift in the position of the beam in a direction orthogonal to the axis of compensation. This limitation could likely be improved by better beam centering on the optics or by implementing a look up table made specifically for astigmatic compensation, or could be corrected for by the use of steering mirrors in the beam path.

The use of the actuators was shown to increase the standard deviation of the measured beam parameters, though this is almost certainly due to the effects of turbulent air flow around the FSHs as a result of their high temperature relative to the environment. These actuators are primarily designed for in-vacuum operation, however, so the turbulence effect does not present a severe limitation on their usefulness. Further studies into the vacuum operation of the actuators, and the impact of the actuators on the quality of the beam transmitted through them are recommended in order to determine the potential for this device to make an impact in achieving the high-power operation of aLIGO. In the future, it may also be interesting to investigate the application of the device presented here as an actuator in a control loop to stabilize mode matching into an interferometer, similar to that described in Ref. [18].

5. Acknowledgments

The authors acknowledge the encouragement of the LIGO Science Collaboration. Prof. Prabir Barooah is also thanked for his helpful discussions. This work is supported by the National Science Foundation under grant under grants PHY-0855313 and PHY-12055FSH12. This paper has been assigned the LIGO document No. LIGO-P1300045.

References

- [1] J. D. Foster and L. M. Osterink. "Thermal Effects in a Nd:YAG Laser". *Journal of Applied Physics*, 41:3656–3663, August 1970.
- [2] C. E. Greninger. "Thermally induced wave-front distortions in laser windows". *Appl. Opt.*, 25:2474–2475, August 1986.
- [3] P. Hello and J-Y. Vinet. "Analytical models of transient thermoelastic deformations of mirrors heated by high power cw laser beams". *J. Phys. France*, 51(20):2243–2261, 1990.
- [4] M. A. Arain, W. Z. Korth, L. F. Williams, R. M. Martin, G. Müller, D. B. Tanner, and D. H. Reitze. "Adaptive control of modal properties of optical beams using photothermal effects". *Optics Express*, 18:2767, January 2010.
- [5] R. Schmiedl. "Adaptive optics for CO₂ laser material processing". In *2nd International Workshop on Adaptive Optics for Industry and Medicine*, pages 32–36. World Scientific Publishing, 2000.
- [6] Susumu Sato. "Liquid-crystal lens-cells with variable focal length". *Japanese Journal of Applied Physics*, 18(9):1679–1684, 1979.
- [7] D. P. Jablonowski and S. H. Lee. "A coherent optical feedback system for optical information processing". *Applied Physics*, 8:51–58, September 1975.
- [8] T. L. Kelly, A. F. Naumov, M. Y. Loktev, M. A. Rakhmatulin, and O. A. Zayakin. "Focusing of astigmatic laser diode beam by combination of adaptive liquid crystal lenses". *Optics Communications*, 181:295–301, July 2000.
- [9] Gregory M Harry and the LIGO Scientific Collaboration. "Advanced LIGO: the next generation of gravitational wave detectors". *Classical and Quantum Gravity*, 27(8):084006, 2010.
- [10] L. Winkelman, O. Puncken, R. Kluzik, C. Veltkamp, P. Kwee, J. Poeld, C. Bogan, B. Willke, M. Frede, J. Neumann, P. Wessels, and D. Kracht. "Injection-locked single-frequency laser with an output power of 220 W". *Applied Physics B: Lasers and Optics*, 102:529–538, 2011. 10.1007/s00340-011-4411-9.
- [11] M. A. Arain. "A note on substrate thermal lensing in the input mode cleaner". LIGO internal note T070095-00-E, 2007. <https://dcc.ligo.org/public/0027/T070202/000/T070202-00.pdf>
- [12] D. Michel, T. Graf, H. J. Glur, W. Lüthy, and H. P. Weber. "Thermo-optically driven adaptive mirror for laser applications". *Applied Physics B: Lasers and Optics*, 79:721–724, October 2004.
- [13] M. A. Arain, V. Quetschke, J. Gleason, L. F. Williams, M. Rakhmanov, J. Lee, R. J. Cruz, G. Mueller, D. B. Tanner, and D. H. Reitze. "Adaptive beam shaping by controlled thermal lensing in optical elements". *Appl. Opt.*, 46:2153–2165, April 2007.
- [14] R. Lawrence, D. Ottaway, M. Zucker, and P. Fritschel. "Active correction of thermal lensing through external radiative thermal actuation". *Optics Letters*, 29:2635–2637, November 2004.
- [15] J. Schwarz, M. Geissel, P. Rambo, J. Porter, D. Headley and M. Ramsey. "Development of a variable focal length concave mirror for on-shot thermal lens correction in rod amplifiers", *Optics Express*, 14:10957–10969, November 2006.
- [16] Product of Allied Vision Technologies, model number gc780, working at mono 8 mode.
- [17] E. Morrison, D. I. Robertson, H. Ward, and B. J. Meers. "Automatic alignment of optical interferometers". *Appl. Opt.*, 33:5041–5049, August 1994.
- [18] G. Mueller, Q. Shu, R. Adhikari, D. B. Tanner, D. Reitze, D. Sigg, N. Mavalvala, and J. Camp.

“Determination and optimization of mode matching into optical cavities by heterodyne detection”.

Opt. Lett., 25(4):266–268, Feb 2000.